

Ideal Sensor Chips —A Smart Microsensor Chip with LSI and MEMS Process and Materials—

Makoto Ishida*

Toyohashi University of Technology, 1-1 Hibarigaoka Tempaku, Toyohashi, Aichi 441-8580, Japan

(Received October 11, 2017; accepted November 15, 2017)

Keywords: sensor chip with LSI, CMOS and MEMS process, SOI material and devices, VLS probe chip, pH image sensor

The sensor chips developed in Toyohashi University of Technology and the facility called the “LSI factory” since 1979 were reviewed. The original and unique devices were fabricated using not only the standard Si-LSI process and materials, but also the MEMS process and materials. Researchers including students can fabricate their own devices by themselves, which could lead to the production of original prototype devices using special processes and materials together with the CMOS process. Demonstrating the devices is more persuasive than theoretically explaining them in this manuscript. Aside from its educational use, this explains the existence of the LSI factory in Toyohashi University.

1. Introduction

Since 1979, Professor Nakamura and a semiconductor device research group including me, in Toyohashi University of Technology (founded by the government in 1976), attempted to establish an ideal integrated circuit (IC) facility from the design to IC processes (bipolar and MOS) for evaluation. For 37 years, we continued to improve and maintain this LSI, sensor, and MEMS facility, which is called the “LSI factory”, which is not a real factory, but an LSI and sensor/MEMS fusion-fabrication research center (Electron Device Research Center: EDRC). It is important to show and explain a new device not only by discussing it in a manuscript but also by fabricating a prototype device. Also in the center, no standard CMOS process and materials can be used, so a unique device could be fabricated, and CMOS and MEMS processes are combined; combining both processes at the same place is difficult. Unique sensors were developed at the early stage until 2000 as shown in Fig. 1, examples of which were a monolithic preamplifier for detecting brain waves of swimming carp for space sickness study in an Endeavor space shuttle experiment as shown in Fig. 2,⁽¹⁾ a three-dimensional accelerometer chip with 5 μm CMOS-LSI,⁽²⁾ and a lab-on chip for the measurement of hemoglobin in human blood.⁽³⁾

Until now, important projects such as 21th Center of Excellence (COE: 2002–2007), Global COE (2008–2013), and the Research University Project (2013–2023) supported by Japan

*Corresponding author: e-mail: ishida@ee.tut.ac.jp
<https://doi.org/10.18494/SAM.2018.1773>

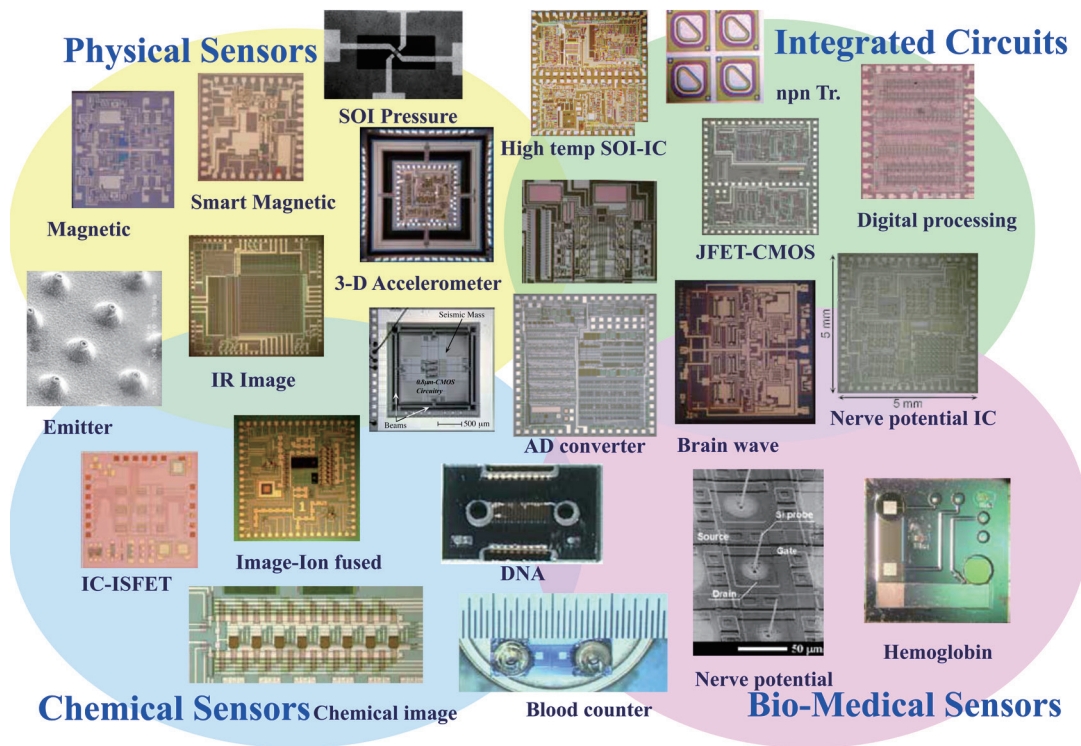


Fig. 1. (Color online) Smart microchips developed in Toyohashi University of Technology (TUT) (1979–2000).

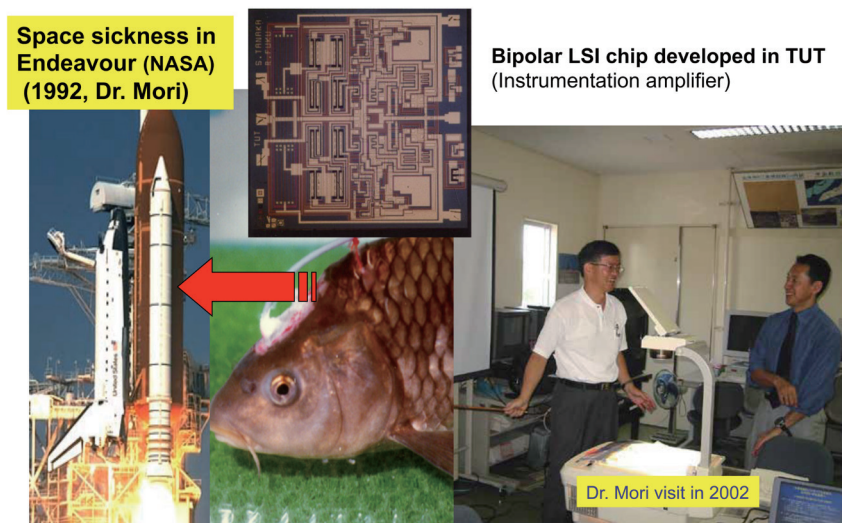
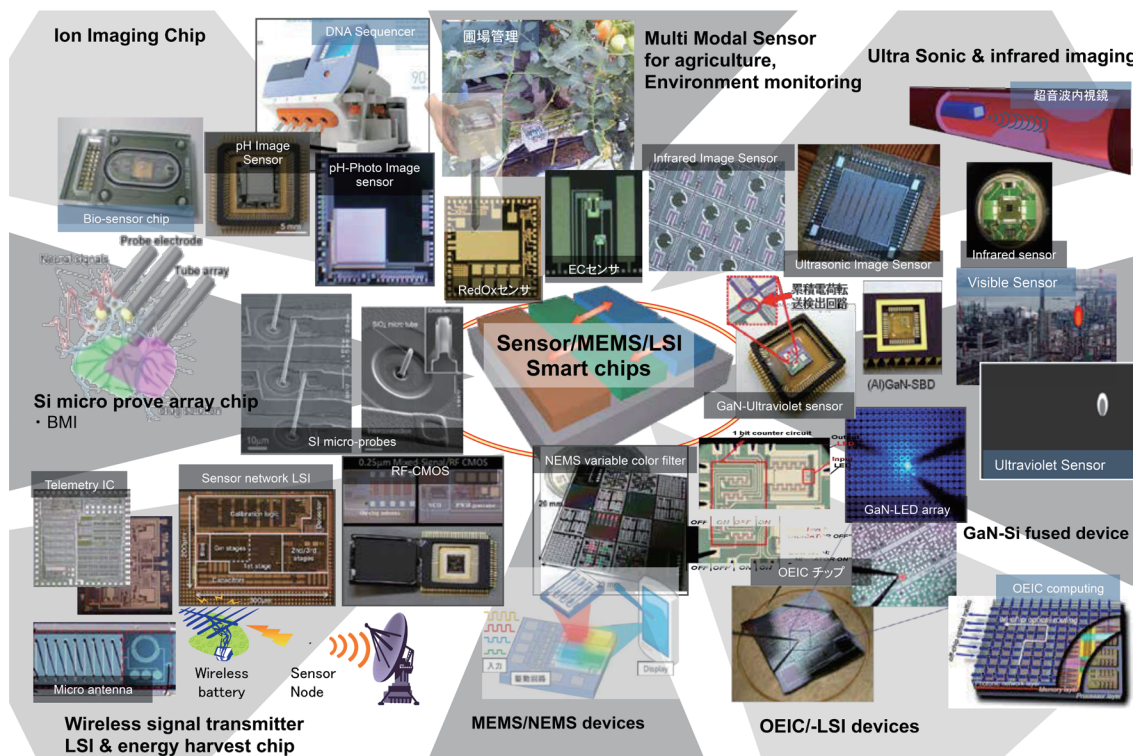


Fig. 2. (Color online) First chip developed from TUT, Endeavour Experiment by Dr. Mori (1980–1992).

Government have been carried out using the center as a core facility. Also, Electronics-Inspired-Interdisciplinary Research Institute (EIIRIS)⁽⁴⁾ was established in 2013 including the LSI factory shown in Fig. 3 as the first research institute in our university to promote the interdisciplinary research with sensors, MEMS, and LSI.



(a)



(b)

Fig. 3. (Color online) (a) LSI Fab Center in EIIRIS: LSI, sensors and MEMS. (b) Smart sensing chips developed in EIIRIS.

2. Silicon-on-Insulator (SOI) Materials for Smart Sensors

The epitaxial insulator γ -Al₂O₃ on Si substrates, as shown in Fig. 4, was developed as an SOI material, and new devices and sensor applications with Si-LSI were proposed.^(5,6) The insulator thin film was used for the first sensor device to fabricate diaphragm structures as an etching stop layer, and high-temperature pressure sensors were developed using double SOI structures of Al₂O₃ and Si.⁽⁷⁾ Then, very thin γ -Al₂O₃ crystalline insulator layers of a few nm thickness were used for new devices such as a resonance tunnel diode, a MOS device with a high-k gate, and a MIS field-emission device as shown in Fig. 5.⁽⁸⁻¹⁰⁾ Integration processes of γ -Al₂O₃/Si substrates and CMOS circuits were studied using ferroelectric materials for IR image sensors

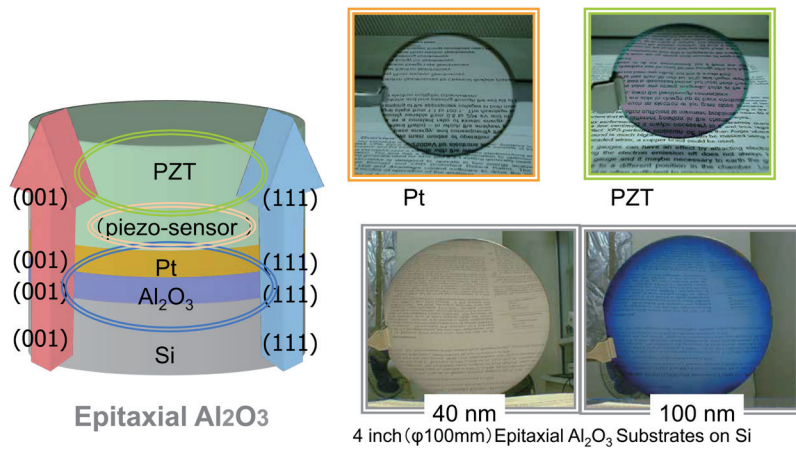


Fig. 4. (Color online) Multipitaxial thin films (Pt, PZT) on Si with Al₂O₃.

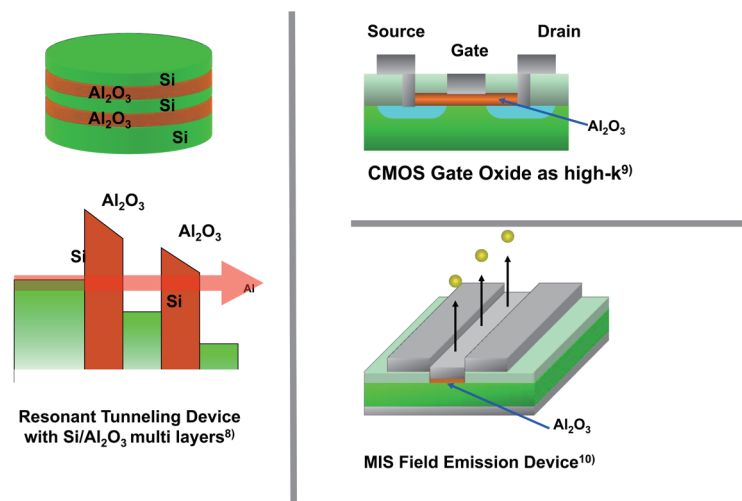


Fig. 5. (Color online) Ultrathin crystalline Al₂O₃ on Si substrates and devices fabricated by molecular beam epitaxy (MBE).

and piezoelectric micromachined ultrasonic transducer (pMUT) arrays in Fig. 6, which use epitaxial lead zirconate titanate (PZT) and Pt films on epitaxial γ -Al₂O₃/Si substrates to integrate with Si-LSI and improve the sensitivity compared with polycrystalline PZT films. The epitaxial γ -Al₂O₃ film not only controls the orientation of PZT films but also shows thermally and chemically stable properties and good barrier properties of Pb diffusion into the Si substrate from PZT.^(11–14) Furthermore, the γ -Al₂O₃ film contains only Al and O, which are CMOS materials, not rare-earth materials. Hence, a γ -Al₂O₃ film is a suitable material for a buffer layer, instead of conventional SiO₂ films, for the monolithic integration of the pMUT array and signal processing circuitry.

3. Toyohashi Probes: A Si Needle Electrode Array Formed by Vapor–Liquid–Solid (VLS) Growth

One of our developed smart chips is a smart silicon microprobe array chip to record neural activities for analyzing the mechanism of the retina and brain, or for neural interfacing. Our group proposed the microelectrode array chip with extremely fine, in other words, poorly invasive silicon probes of 1–2 μ m diameter, and fabricated it using the standard CMOS process followed by the selective VLS growth method.^(15,16) Figure 7 indicates an ideal smart microprobe array chip for this application. Using the chip (Toyohashi Probes), the feasibility of *in vitro* recording of neural activities in a carp retina and *in vivo* recording of the peripheral nervous activity of a rat was demonstrated.

An ideal heterogeneous integration chip of vertically aligned extracellular microscale silicon (Si) probe arrays on (111)Si was demonstrated with MOSFET amplifiers on (100)Si, by IC processes and subsequent VLS growth of Si probes. To improve the extracellular recording capability of the microprobe with a high impedance of >1 M Ω at 1 kHz, here we integrated (100)Si source follower buffer amplifiers by \sim 700 $^{\circ}$ C VLS growth-compatible (100)Si MOSFET technology as shown in Fig. 8. Without an on-chip source follower, the output/input signal

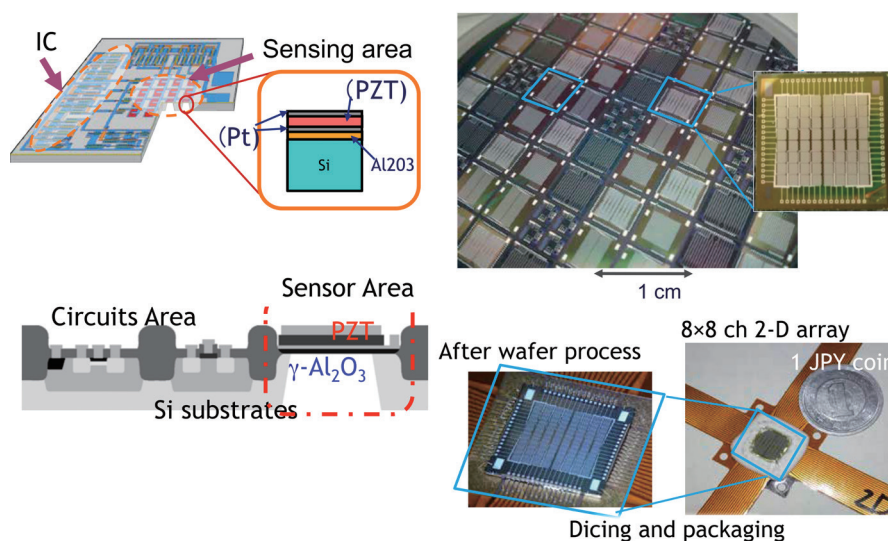


Fig. 6. (Color online) Imaging sensors using SOI structures of Al₂O₃/Si.

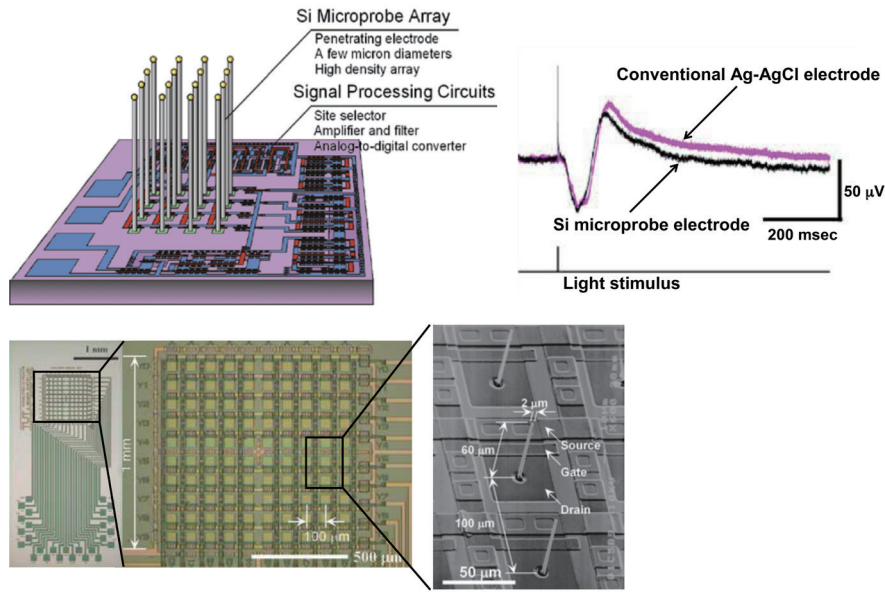


Fig. 7. (Color online) Microprobe electrode array chip with IC.

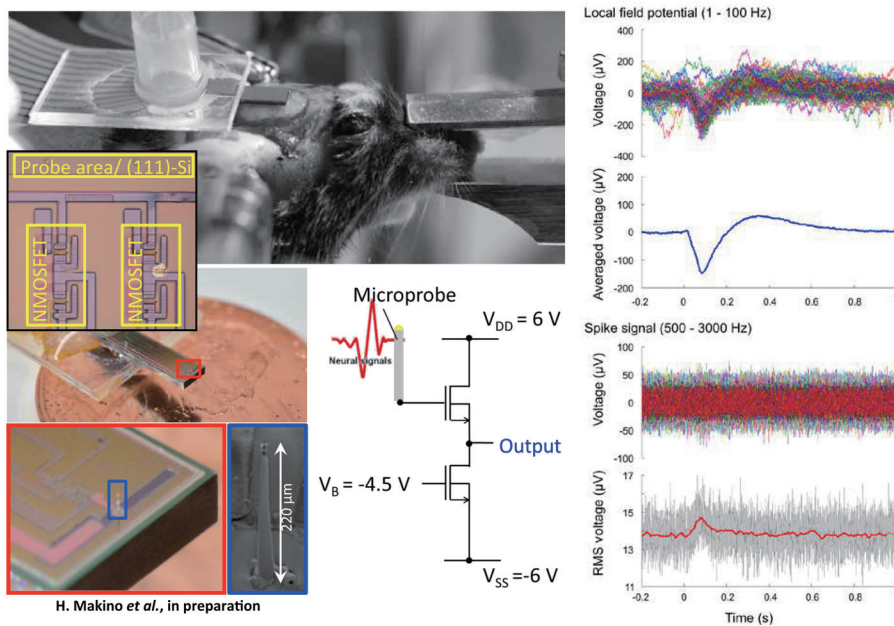


Fig. 8. (Color online) Microscale Si probe arrays on (111)Si with MOSFET amplifiers on (100)Si.

ratio of the microprobe in saline was 0.59, which was improved to 0.72 by the on-chip source follower configuration, while the signal-to-noise ratio (SNR) was improved to 12.5 dB at the frequency of extracellular recording. These results indicate that the integration of the source follower buffer amplifiers is highly efficient for enhancing the performance of high-impedance microprobe electrodes in neural recordings.⁽¹⁷⁾

To approach deep cell layers in a cortex, microneedles should be longer than 400 μm (e.g., $\approx 400 \mu\text{m}$ for the cortical layer IV in the mouse brain and the cortical layer II in the human brain). We propose the use of a dissolvable silk-based scaffold to enhance the stiffness of the high-aspect-ratio flexible microneedles as shown in Fig. 9.⁽¹⁸⁾ The needle of 550 μm length penetrated into the brain without buckling.

The *in vivo* recording capability of the device is demonstrated using mice, and spike signals with peak-to-peak amplitudes of 200–300 μV in the 0.5–3 kHz range are stably detected as shown in Fig. 10, including single-unit activities in cortical layer 2/3. In addition, the device

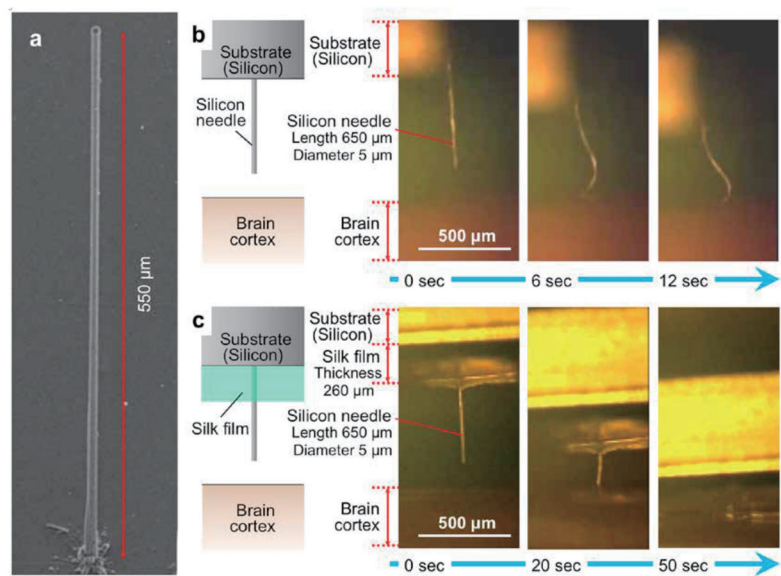


Fig. 9. (Color online) Long Si needles of more than 400 μm length and a few μm diameter.

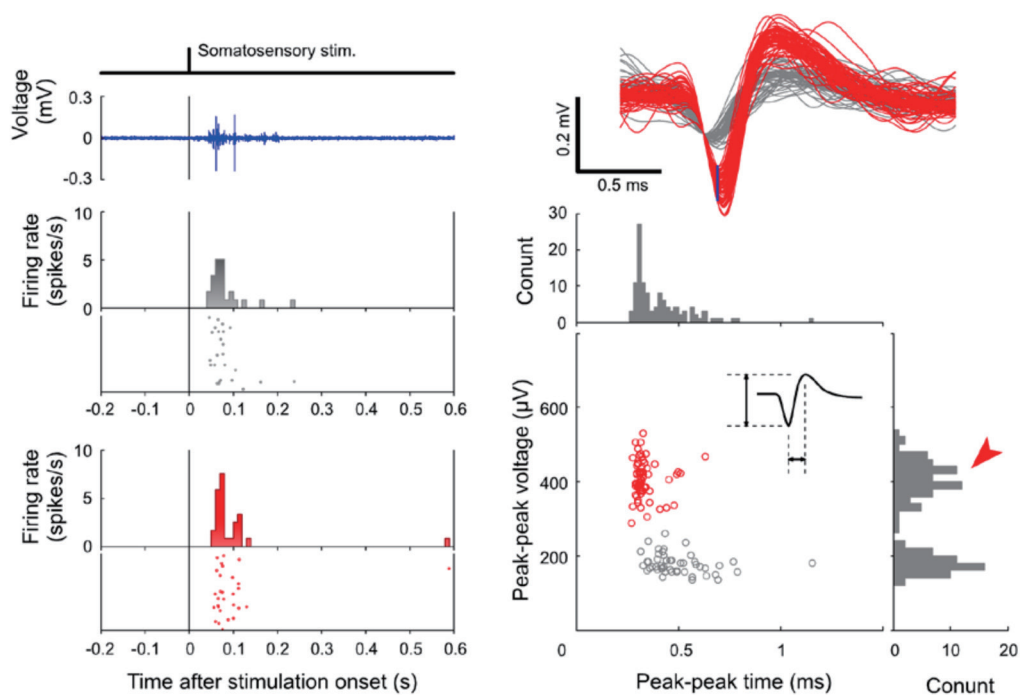


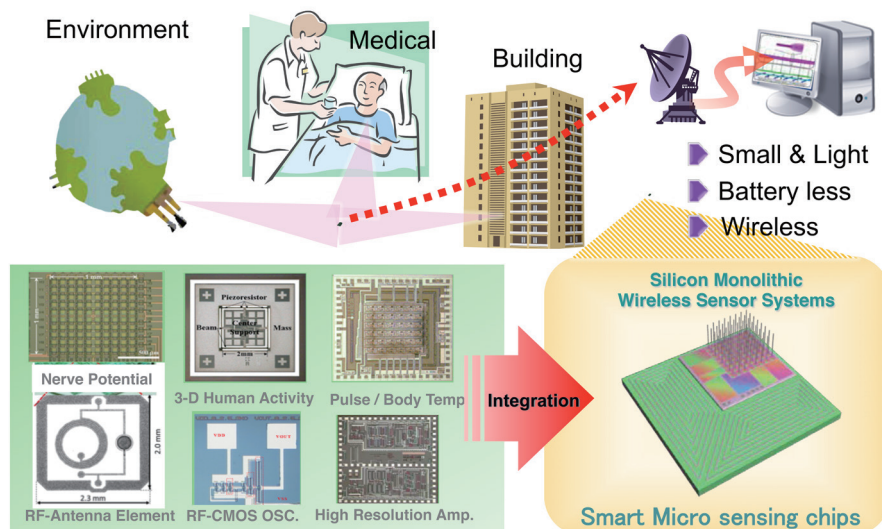
Fig. 10. (Color online) *In vivo* neuronal recording from a mouse somatosensory cortex.

packaged with a flexible PCB shows stable unit recordings for 98.5 min ($n = 4$). Consequently, our modular, low-invasive needle electrode block devices present an effective route for single-unit recordings *in vivo*, as well as demonstrating adaptability in a device design for a diverse range of experiments.⁽¹⁹⁾ The needle electrodes used in this study have a length of 160 μm , which is sufficient to reach mouse layer 2/3. Since mouse layer 1 consists of only a few neurons, it can be deduced from the unit-activity recordings that the electrodes reach mouse layer 2/3. In addition, the thicknesses of mouse layers 1 and 2/3 are about 100 and 200–300 μm , respectively, therefore eliminating the possibility of signal detection from mouse layer 4.

These results indicate that the Toyohashi probes can easily penetrate, are very low invasive electrodes, and enable a long stable recording, which result in the possibility of detecting signals immediately after needle penetration.

4. Smart Microsensing Chips

The integration of RF transmitter technology with CMOS/MEMS microsensors (a smart microsensor) is required to realize a wireless smart microsensor system as shown in Fig. 11. The integration techniques for fully integrated smart microsensor systems were developed. Voltage-controlled oscillators (VOCs) have been designed and fabricated for the 300 MHz frequency band by our CMOS fabrication technology. Also, on-chip spiral inductors for the LC resonator and an integrated antenna have been fabricated with a CMOS-compatible metallization process.^(20,21) A low-radiation-loss on-chip antenna using a sapphire substrate was proposed to improve the antenna gain. The fabricated antenna has a return loss of approximately -3.58 dB at the center frequency of 360 MHz. The on-chip antenna using a sapphire substrate achieves a 12.9 dB higher gain and can markedly reduce the power consumption of the transmitter by 95% compared with that using a silicon substrate.⁽²²⁾ We demonstrate signal transmission using the proposed on-chip antenna and a CMOS transmitter chip. Figure 12 shows the fabricated transmitter device connected by wire bonding and the measurement system for



Sensor + wireless battery • transmitter + AD circuits

Fig. 11. (Color online) Smart microsensing chip.

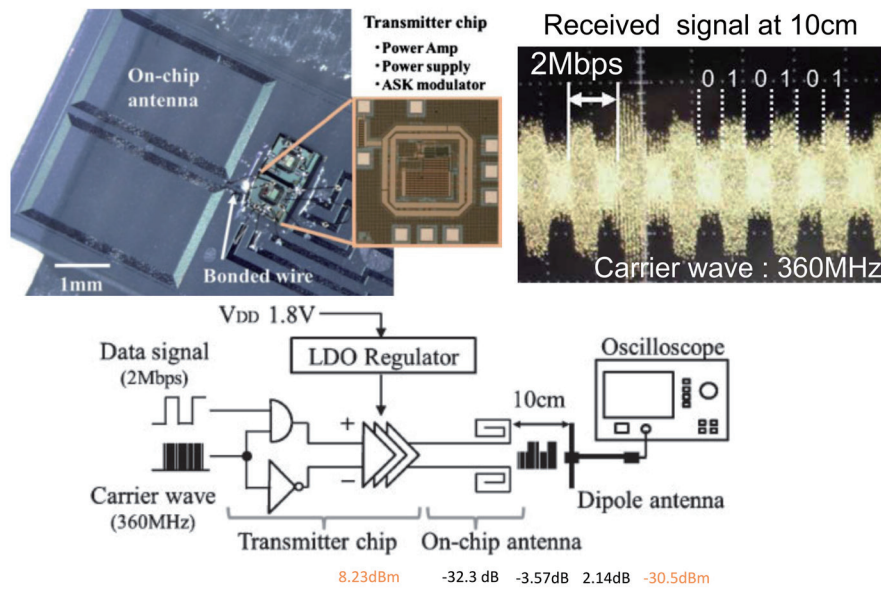


Fig. 12. (Color online) Transmission demonstration of 360 MHz wave by transmitter device with chip antenna connected by wire bonding and the measurement system for transmission demonstration.

transmission demonstration. The transmitter chip has a size of $700 \times 700 \mu\text{m}^2$ and includes a power amplifier, a power supply, and an amplitude shift keying (ASK) modulator. The data signal of 2 Mbps and the carrier wave of 360 MHz were input into the transmitter chip. The ASK-modulated differential output signal was applied to the antenna. In this measurement, the emitted radio wave was received using a dipole antenna at a distance of 10 cm. In Fig. 12, the received signal waveform is shown. A low or high digital signal level was observed from this received signal waveform. The total power consumption of the system was 6.66 mW and the received power was $0.88 \mu\text{W}$. The fabricated antenna is therefore considered suitable as a data transmission antenna in implantable wireless medical systems.

5. Ion Image Sensors

By using the charge-transfer-type pH sensor, a pH image sensor, capable of measuring two-dimensional distributions of chemical reactions, has been proposed by Sawada *et al.*⁽²³⁾ A prototype image sensor has been successfully fabricated in the center, and the 2-D dynamic imaging of the pH of a solution was successfully performed as shown in Fig. 13. It was confirmed that the real-time imaging of a chemical reaction was performed with the pH image sensor. The dynamic measurement, which means to observe in real time, is important to determine the variation in the pH of a solution over time. Moreover, as the proposed sensor was able to observe a 2-D dynamic pH image, spatial information was obtained. This prototype device (32×32 array)⁽²⁴⁾ was very useful and important for researchers including industry persons to understand and know the possible applications of such a new device, especially for interdisciplinary researchers. Since this successful result, the image sensor has been developed

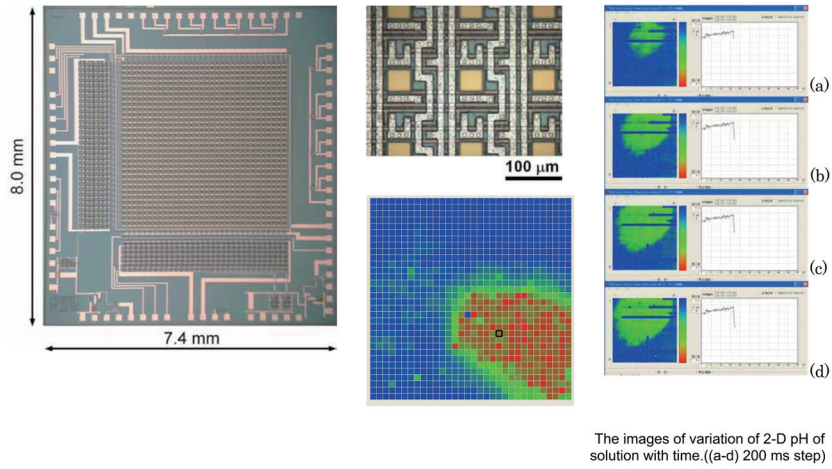
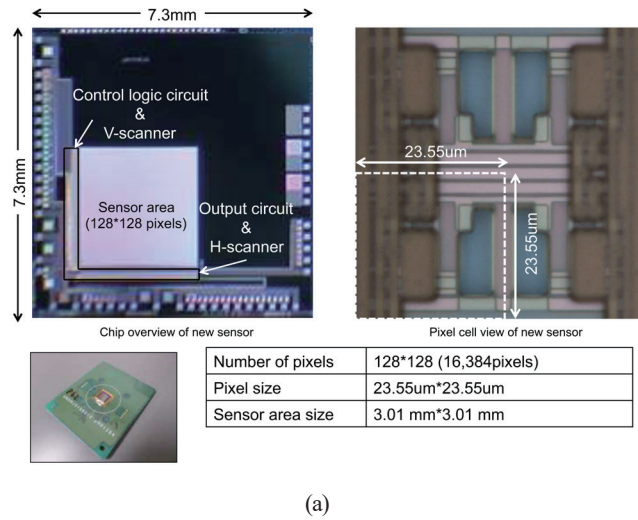
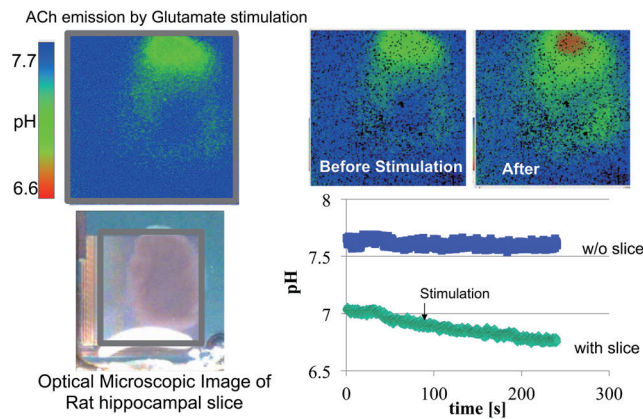


Fig. 13. (Color online) 32 × 32 pH image sensor and 2-D dynamic pH image with visible one.



(a)



(b)

Fig. 14. (Color online) (a) Photo and pH fused image sensor chip. (b) ACh emission in the cortical slice. Label-free ACh imaging was successfully carried out.

with industry work, and current pH image sensors consist of 128×128 pixels, each with a sensing area of $10 \times 25 \mu\text{m}^2$, as shown in Fig. 14(a). A pH imaging consortium started to address issues related to ion image sensing. Future plans may include pH imaging devices for visualizing the movement and distribution of other ions including calcium and sodium. Sawada and coworkers have reported the use of the sensor for the real-time imaging of acetylcholine (ACh) enzyme reactions, as shown in Fig. 14(b),^(25,26) and image changes in the distribution of ACh when nerve cells are stimulated with KCl.

6. Conclusions

The sensor chips developed since 1979 in the LSI center were original and unique, and used not only the standard Si-LSI process and materials, but also the MEMS process and materials. To improve and maintain the facility, the LSI center called the LSI factory was developed and resulted in EIIRIS in 2010. Researchers including students can fabricate their own devices by themselves, which could lead to the production of original prototype devices using special processes and materials together with the CMOS process. To explain the properties of the new devices, the operation of the prototype devices, which can demonstrate the principle of the original devices, is more persuasive than the explanation of the principle in this manuscript. Aside from its educational use, this explains the existence of the LSI factory in Toyohashi University.

Acknowledgments

Many thanks to all contributing researchers and staff who work with me for 37 years, especially the late Professor T. Nakamura who encouraged me to go into the LSI technology field and supported my work endlessly, so I could concentrate on the above-mentioned research and continue to develop and maintain the “LSI facility” after he retires. The research results described here are the results of the Integrated Research Group (ICG: <http://int.ee.tut.ac.jp/icg/wp/en/>), which is a Si-based semiconductor research group of about 70 people every year, who are Professor K. Sawada, Mr. M. Ashiki, Associate Professor T. Kawano, Dr. D. Akai, Dr. I. Akita, Professor H. Takao, and other many colleagues and staff including ICG students.

References

- 1 T. Nakamura, M. Ishida, S. Tanaka, M. Ashiki, S. Usui, S. Takagi, A. Takabayashi, S. Mori, and S. Watanabe: *Environ. Med.* **29** (1983) 107.
- 2 H. Takao, Y. Matsumoto, and M. Ishida: *IEEE Trans. Electron Devices* **46** (1999) 100.
- 3 T. Noda, H. Takao, M. Ashiki, H. Ebi, K. Sawada, and M. Ishida: *Jpn. J. Appl. Phys.* **43** (2004) 2392.
- 4 EIIRIS: <http://www.eiiris.tut.ac.jp> (accessed November 15, 2017)
- 5 M. Ishida, I. Katakabe, T. Nakamura, and N. Ohtake: *Appl. Phys. Lett.* **52** (1988) 1326.
- 6 M. Ishida, S. Yamaguchi, Y. Masa, and T. Nakamura: *J. Appl. Phys.* **69** (1991) 8408.
- 7 Y. T. Lee, H. Takao, and M. Ishida: *Sens. Mater.* **17** (1995) 269.
- 8 M. Shahjahan, Y. Koji, K. Sawand, and M. Ishida: *Jpn. J. Appl. Phys.* **41** (2002) 2602.
- 9 T. Okada, K. Sawada, M. Ishida, and M. Shahjahan: *Appl. Phys. Lett.* **85** (2004) 5004.
- 10 J. S. Kim, M. Shahjahan, H. K. Mosammat, K. Sawada, and M. Ishida: *Jpn. J. Appl. Phys.* **45** (2006) 5107.

- 11 D. Akai, M. Yokawa, K. Hirabayashi, K. Matsushita, K. Sawada, and M. Ishida: *Appl. Phys. Lett.* **86** (2005) 202906.
- 12 D. Akai, K. Ozaki, Y. Numata, K. Suzuki, N. Okada, and M. Ishida: *Jpn. J. Appl. Phys.* **51** (2012) 11PA04.
- 13 K. Oishi, D. Akai, and M. Ishida: *Solid-State Electron.* **103** (2015)110.
- 14 D. Takashima, K. Ozaki, M. Nishimura, N. Okada, D. Akai, and M. Ishida: *Sens. Mater.* **27** (2015) 1.
- 15 M. Ishida, K. Sogawa, A. Ishikawa, and M. Fujii: *Transducers '99, Digest of Technical Papers* **2** (1999) 866.
- 16 T. Kawano, Y. Kato, R. Tani, H. Takao, K. Sawada, and M. Ishida: *IEEE Trans. Electron Devices* **51** (2004) 415.
- 17 H. Makino, K. Asai, M. Tanaka, S. Yamagiwa, H. Sawahata, I. Akita, M. Ishida, and T. Kawano: *MEMS* **2015** (2015) 686.
- 18 S. Yagi, S. Yamagiwa, Y. Kubota, H. Sawahata, R. Numano, T. Imashioya, H. Oi, M. Ishida, and T. Kawano: *Adv. Healthcare Mater.* **4** (2015) 1949.
- 19 H. Sawahata, S. Yamagiwa, A. Moriya, T. Dong, H. Oi, Y. Ando, R. Numano, M. Ishida, K. Koida, and T. Kawano: *Sci. Rep.* **6** (2016) 35806.
- 20 J. W. Kim, H. Takao, K. Sawada, and M. Ishida: *IEEJ Trans. Electr. Electron. Eng.* **2** (2007) 365.
- 21 M. Sudou, H. Takao, K. Sawada, and M. Ishida: *Sens. Actuator, A* **145–146** (2008) 343.
- 22 K. Okabe, I. Akita, and M. Ishida: *Jpn. J. Appl. Phys.* **53** (2014) 04EL09.
- 23 K. Sawada, T. Shimada, T. Ohshima, H. Takao, and M. Ishida: *Sens. Actuators, B* **98** (2004) 69.
- 24 T. Hizawa, J. Matsuo, T. Ishida, H. Takao, H. Abe, K. Sawada, and M. Ishida: *Transducers' 2007* **2** (2007) 1311.
- 25 S. Takenaga, Y. Yamai, K. Okumura, M. Ishida, and K. Sawada: *Jpn. J. Appl. Phys.* **51** (2012) 027001.
- 26 T. Sakurai, A. Iwashita, K. Okumura, M. Ishida, and K. Sawada: *Transducers' 2013* (2013) 760.